Carbon isotope chemostratigraphy of the Late Ordovician (Hirnantian) Keel Oolite and the Silurian Cochrane, Clarita, and lowermost Henryhouse formations in the Arbuckle Mountains, Oklahoma, USA

Mikael Calner, Rongchang Wu, Guanzhou Yan, Oliver Lehnert & Thomas M. Stanley

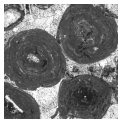

Marine carbonate oolites are a key feature of the Hirnantian Stage (445.2–443.8 Ma) and their formation may be the combined result of latest Ordovician glacial eustasy and the associated mass extinction event. In this paper, we provide the first highly time-resolved carbon isotope data ($\delta^{13}C_{carb}$) from the Keel Oolite in the Arbuckle Mountains of southern Oklahoma, aiming to clarify its temporal relationship with the overall Hirnantian Isotope Carbon Excursion (HICE) and refine the chronostratigraphy of the oolites in the southwestern United States. However, analyses of the Keel Oolite at the type locality in Holnam quarry, at the classical Highway 77 road-cut, and in the Sunray DX-Davis 1–5 drill core, reveal only a fragmentary carbon isotope record, making any detailed chemostratigraphic correlation of the local Hirnantian difficult. The oolite yields overall consistent $\delta^{13}C$ trend lines and weak to moderate co-variance (R^2 ranging from 0.04–0.49) between carbon and oxygen, indicating no to moderate diagenetic alteration, still they display a *ca.* 1–2‰ offset of the baseline between localities. As there is no firm evidence for any steep increase or decrease in the $\delta^{13}C$ values, it is suggested that the oolites correspond to the peak and plateau interval of the HICE. Brachiopods of the same strata belong in the Edgewood-Cathay Fauna, which normally appears in the time interval corresponding to the falling limb of HICE. At the Highway 77 road-cut, our carbon isotope stratigraphy reaches nine metres into the Silurian succession immediately overlying the oolite, corroborating previous interpretations of an extremely discontinuous stratigraphy with prominent unconformities. Based on the combined information from conodont faunas and our $\delta^{13}C_{carb}$ data, however, we infer or identify the overall position for preserved parts of Silurian $\delta^{13}C$ excursions in the section, including the Late Aeronian Carbon Isotope Excursion (LACIE), the Valgu Carbon Isotope Excursion (Valgu CIE), Early Sheinwoodian Carbon Isotope Excursion (ESCIE), the Mid Homerian Carbon Isotope Excursion (MHCIE), and the Mid Ludfordian Carbon Isotope Excursion (MLCIE). Our geochemical data thus reinforce a modest stratigraphic completeness of the Ordovician-Silurian boundary succession in the Arbuckle Mountains. • Key words: carbon isotope stratigraphy, conodont biostratigraphy, Hirnantian, oolite, *Noixodontus* fauna, Edgewood–Cathay brachiopod fauna.

Calner, M., Wu, R., Yan, G., Lehnert, O. &. Stanley, T.M. 2026. Carbon isotope chemostratigraphy of the Late Ordovician (Hirnantian) Keel Oolite and the Silurian Cochrane, Clarita, and lowermost Henryhouse formations in the Arbuckle Mountains, Oklahoma, USA. *Bulletin of Geosciences 101*(*1*), 173–189 (9 figures, 1 table). Czech Geological Survey, Prague. ISSN 1214-1119. Manuscript received October 19, 2025; accepted in revised form February 28, 2026; published online May 3, 2026; issued May 3, 2026.

Mikael Calner (corresponding author), Department of Earth and Environmental Sciences, Lund University, Sölvegatan 12, SE-223 62 Lund, Sweden; mikael.calner@mgeo.lu.se • Rongchang Wu, State Key Laboratory of Palaeobiology and Stratigraphy, Nanjing Institute of Geology & Palaeontology, Chinese Academy of Sciences, Nanjing 210008, China • Guanzhou Yan, Department of Earth and Environmental Sciences, Lund University, Sölvegatan 12, SE-223 62 Lund, Sweden & State Key Laboratory of Palaeobiology and Stratigraphy, Nanjing Institute of Geology & Palaeontology, Chinese Academy of Sciences, Nanjing 210008, China • Oliver Lehnert, GeoZentrum Nordbayern, Friedrich-Alexander University Erlangen-Nürnberg (FAU), Schlossgarten 5, D-91054, Erlangen, Germany • Thomas M. Stanley, Oklahoma Geological Survey-University of Oklahoma, 100 East Boyd Street, Norman, OK 73019, USA

The Hirnantian Stage is associated with global climatic changes and the Late Ordovician Mass Extinction (LOME; Sheehan 2001, Harper *et al.* 2014, Rasmussen *et al*. 2023). These changes are intimately associated with the Hirnantian Isotope Carbon Excursion (HICE), which to date is documented from many tens, if not more than a hundred, locations around the world and which is an excellent geochemical marker for the event (*e.g.* Brenchley *et al.* 2003, Bergström *et al.* 2014). What is less recognised, at least outside the Ordovician–Silurian research community, is the short-lived and widespread occurrence of an unusual limestone type during this time

interval (Amsden & Barrick 1986, Calner & Lehnert 2009, Wang *et al.* 2017). These oolites, which are formed principally through inorganic carbonate precipitation but likely in tandem with microbial processes that catalyze precipitation (*e.g*. O'Reilly *et al*. 2017, Li *et al.* 2017) are known from North America, Baltoscandia and South China, and formed a circum-tropical belt during the mass extinction. Thus, the Hirnantian oolites represent a time-specific facies (*sensu* Brett *et al*. 2012), and likely the combined ecological-sedimentary response to strongly reduced biological carbonate production and post-glacial global warming during the LOME. The reasoning here, which is the topic of a parallel research project, is that mass extinction of shell-bearing biota substantially reduced the marine biological sink for carbonate forming ions. As continental silicate weathering continued to provide crucial ions, and land-to-sea transport potentially increased during the associated eustatic lowstand, the abundance of free carbonate forming ions and marine alkalinity built up. This resulted in an imbalance in ocean-water chemistry that promoted a short-lived buffering pulse of inorganic carbonate precipitation during the Hirnantian post-glacial warming and transgression. The resulting oolites have a particularly wide distribution in southern Laurentia. They are documented from several states of western and south-central United States, including the Hanson Creek Oolite of Nevada (Finney *et al.* 1999, LaPorte *et al.* 2009), the Keel Oolite and Pettit Oolite, both of Oklahoma (Amsden & Barrick 1986), Cason Oolite of Arkansas (Craig 1969, Lemastus 1979, Amsden & Barrick 1986), the Leemon Oolite of Missouri (Amsden & Barrick 1986, Bergström *et al*. 2006) and the Noix oolite from eastern Missouri (Bergström & Boucot 1988). These oolites are thin units that rarely exceed a few meters in thickness and are often bound by unconformities. Based on conodont biostratigraphy, specifically the *Noixodontus* fauna, and the presence of brachiopods of latest Ordovician age (Amsden 1974), they can be confidently tied to the Hirnantian Stage. A more precise intra-Stage age determination has proved difficult (see Amsden & Barrick 1986 for a regional discussion), but in the most recent analysis of Hirnantian brachiopod faunas globally, the Keel assemblage was included in the new Edgewood–Cathay Fauna. This fauna may entirely succeed the well-known *Hirnantia* Fauna, suggesting a latest Hirnantian age for the local oolite formation (Rong *et al*. 2020). The finer detail of this stratigraphic interval is long recognized as difficult to study also due to several erosional and non-depositional hiatuses. Bergström & Boucot (1988) summarized the then-known localities exposing this interval in the United States and concluded that there are few conformable successions across the O–S boundary in cratonic successions with limestone facies. They noted, however, that such hiatuses were likely to be relatively less important in the southern mid-continent.

In this paper, we document the lithostratigraphy and carbon isotope stratigraphy of the Keel Oolite of southern Oklahoma. It crops out in several natural sections and road-cuts in the Arbuckle Mountains, is exposed in abandoned or active quarries throughout south-central Oklahoma and is known from drill cores throughout this area (Amsden 1957, 1959; Amsden & Barrick 1986; Stanley 2001). The principal aim of our research is to study the temporal relationship between the HICE and the Keel Oolite to understand the degree of stratigraphical completeness of this distinct unit, and to test the usage of highly time-resolved $\delta^{13}C_{carb}$ stratigraphy for the local to regional correlation of this limestone. The rationale is that HICE is not only a prominent geochemical marker for the Hirnantian Stage but also may help to reveal the finer details of the stage, by utilizing the rising limb, peak and plateau, and falling limb of the anomaly as segments of correlative time (as first employed by Brenchley *et al.* 2003).

Geological setting and stratigraphy

The Arbuckle Mountains of southern Oklahoma form a low-relief inlier of folded and faulted Precambrian and Palaeozoic rocks (Ham 1969, Stanley 2001; Fig. 1). The outcropping lower Palaeozoic succession is dominantly carbonate rocks that have been quarried in outcrops and that are exposed in numerous natural outcrops and along the roads, not least in impressive exposures along Highway 77, which transects the Arbuckle anticline from south to north. The herein studied succession belongs to the Hunton Group, which constitutes mainly fossiliferous limestones that formed along a subtropical shallow carbonate ramp setting beginning in the Late Ordovician and continuing through the Early Devonian. The Keel Oolite represents the basal unit of the Hunton Group, and its upper boundary marks the unconformable Ordovician–Silurian boundary in the area. The Keel is predominantly an oolitic grainstone with local occurrences of bioclastic grainstone and packstone at its base. It is unconformably bounded, at least in the area of the outcrop belt, by the mid–upper Katian Sylvan Shale below and the lower Silurian (upper Aeronian–Telychian) Cochrane Limestone above (*e.g.* Amsden 1957, 1959; Fig. 2). Throughout most of this area, the Keel Oolite maintains a thickness between 0.3 and 0.6 m. A maximum thickness of 4.6 m for the Keel Oolite occurs along the eastern part of the outcrop belt, southwest of Wapanucka; the no longer accessible section J1 of Amsden (1959) and Amsden & Barrick (1986, p. 16). The stratigraphic subdivision of the Keel Oolite has been discussed in detail by Amsden (1959, pp. 30–44) and Amsden & Barrick (1986). They distinguished a lower member composed of bioclastic packstone–grainstone (the

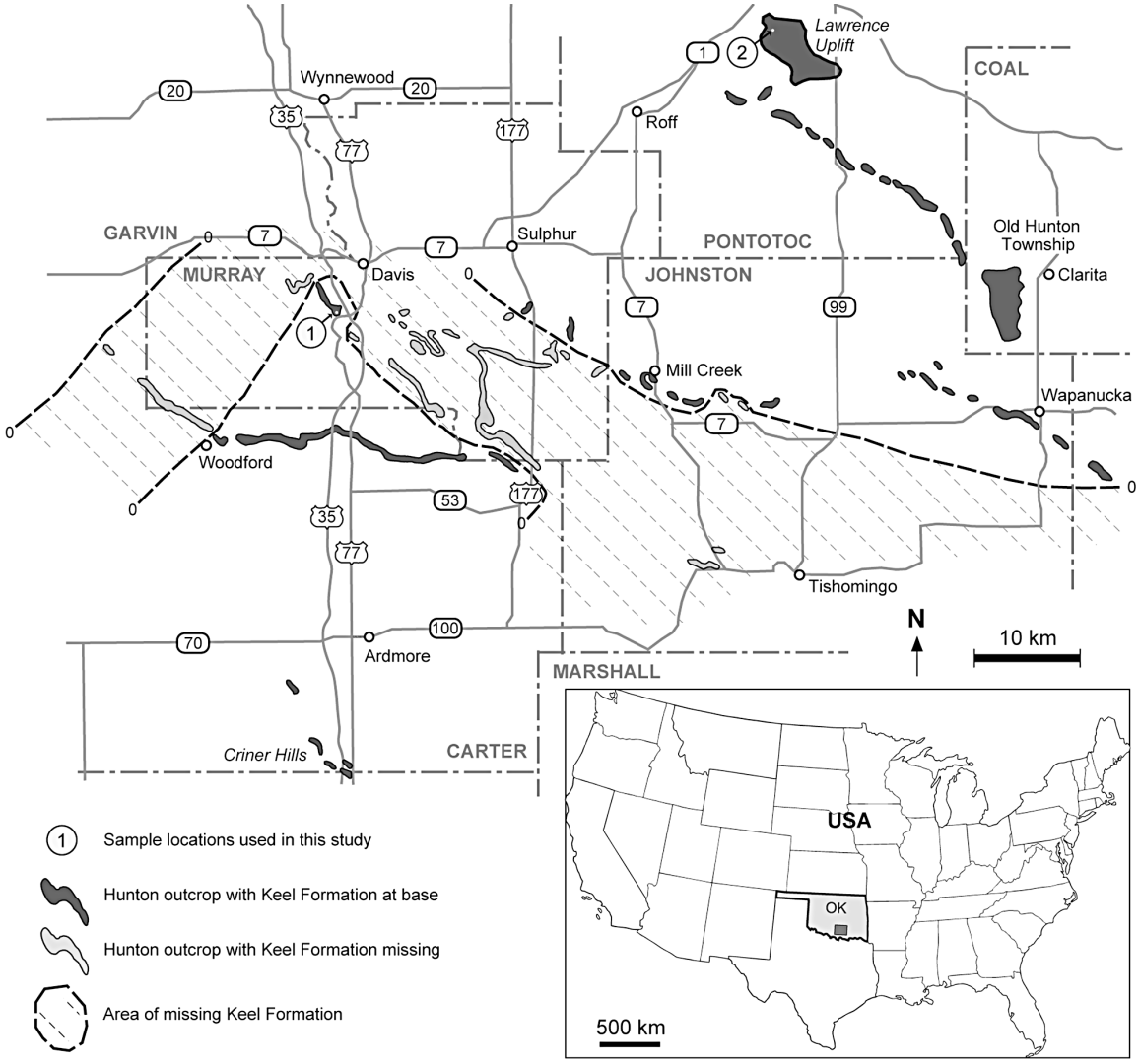

Figure 1. Map showing the Arbuckle Mountain area of south-central Oklahoma and the distribution of Hunton Group exposures with and without the presence of the Keel Oolite. Note that the Keel is cut out by erosion within a large area (thin stippled lines) and that its greatest thickness, around 5 m, is in the area between Wapanucka, Clarita and the Lawrence uplift in the eastern part of the map area. Locality 1 is the classical road-cut locality named Highway 77 (Stop 8 of Stanley 2001), and locality 2 is within the active Ada Aggregate Quarry in the Lawrence uplift, previously referred to as either Holnam quarry or Lawrence quarry (Amsden & Barrick 1986; Stop 2 of Stanley 2001). The Sunray DX-Davis 1–5 drill core was drilled outside the area of the map, near the Canadian River, *ca.* 32 km northeast of our locality 2 in the Lawrence uplift. Figure adapted from figure 12 of Amsden (1959, p. 34).

Ideal Quarry Member) overlain by two separate oolite units ('lower and upper Keel oolites') that locally, in a few localities, are separated by a laminated limestone. In this study, we also sampled the overlying Cochrane, Clarita (including the Prices Falls and Fitzhugh members) and basal Henryhouse formations at the Highway 77 road-cut to understand the succession immediately overlying the Keel Oolite. This succession (Fig. 2) has been described in good detail by Amsden (1959), Barrick & Klapper (1976), Amsden *et al*. (1980), Barrick *et al*. (2010a, b), and a detailed account of the sedimentary facies and overall stratigraphy of the outcrop is presented by Stanley (2001).

Unconformities are common in the studied sections and in the Ordovician-Silurian boundary interval of the Arbuckles as a whole. For this reason, the thickness of units may vary greatly within relatively short distances. For instance, the Keel Oolite is locally cut out, and in those areas the Cochrane rests directly on the Sylvan Shale. This evidence of erosion combined with a major biostratigraphic hiatus below the Oolite suggests that the top of the Sylvan Shale formed a relative high in the area before the onlap of the Keel Oolite. In other locations, the Clarita Formation is cut out and the Cochrane is overlain directly by the Henryhouse Formation, or even by Devonian strata. These unconformities have been described by Amsden (1959), and it is beyond the scope of this study to address their significance or origin in terms of eustatic and/or relative (tectonic) sea-level change.

The biostratigraphic age assessment of most of the Keel Oolite is latest Ordovician (Hirnantian) based on diagnostic brachiopod assemblages of the Edgewood–Cathay Fauna (Amsden 1974, Amsden & Barrick 1986, Rong *et al.* 2020) and presence of the distinct *Noixodontus* conodont fauna, which is known from the HICE interval in both Laurentia and Baltica (McCracken & Lenz 1987, Bergström & Boucot 1988, Bergström *et al.* 2006, Männik 2007a; Fig. 2). The genus *Noixodontus*, as well as the type species *Noixodontus girardeauensis* (Satterfield 1971), were originally described from Missouri (McCracken & Barnes 1982). The taxon is now known from several parts of the United States, including the Yukon Territory in Alaska, where it co-occurs with conodonts of the genus *Gamachignathus*, to which a Richmondian age was assigned (Fauna 12) by McCracken & Barnes (1982). Amsden & Barrick (1986) later documented *N. girardeauensis* associated with a Hirnantian brachiopod fauna in the Noix Limestone and therefore suggested a late Gamachian (Fauna 13) age for this species. *N. girardeauensis* also occurs in the Hirnantian of Baltica (Valga-10 and Ruhnu 500 cores, Estonia), where it dominates a low-diversity conodont fauna found in oolites of the Kuldiga Member of the Edole Formation (Nõlvak *et al*. 2006, Männik 2007a). Accordingly, the Hirnantian oolite formation was a short-term event, which recently has been corroborated by zircon dating of uppermost Katian through Rhuddanian graptolite zones (Zhang *et al*. 2025), indicating a duration of individual zones as short as 0.1 to 0.2 My.

Noixodontus girardeauensis has been documented primarily from the lowermost Keel Oolite in several localities in Oklahoma (Amsden & Barrick 1986, p. 57). In the uppermost Keel near the Lawrence uplift, Pontotoc County, Oklahoma, diagnostic elements of *Distomodus* sp. have been recorded, indicating that, locally, the very top of the Keel Oolite is basal Silurian in age (Amsden & Barrick 1986). The oldest Silurian conodont zone of the North American succession, *Distomodus kentuckyensis* Zone, however, is missing in the area, and the Silurian Cochrane Limestone, following directly above the Keel Oolite, normally belongs in the *Dis. staurognathoides* Zone. For the overlying Clarita Formation, we use the conodont data published by Barrick & Klapper (1976, p. 63, tab. 1), as these are the only published data from this formation at the Highway 77 road-cut. The biostratigraphy of the basal part of the Henryhouse Formation has been documented in good detail from the locality by Barrick *et al.* (2010a, b).

Material and methods

Field localities were visited and sampled by MC and TS in May 2023. A total of 122 whole-rock carbon isotope samples were collected from two outcrops and one core section using a handheld micro-drill. The sample series includes HQ1–HQ25 from Holnam quarry (previously named Lawrence quarry and the type locality for the Keel Oolite; see Amsden & Barrick 1986; Stop 2 of Stanley 2001), H1–H77 from the classical and well visited Highway 77 section near Turner Falls and south of Davis (section M17 of Amsden 1959, pp. 256–258; Stop 8 of Stanley 2001; Stop 6 of Carlucci *et al*. 2015), and SDX1-SDX20 from the Sunray DX-Davis 1–5 drill core (Hughes County, WGS84 coordinates 34.90698 −96.48999; core boxes 1–8, corresponding to 3818–3842 ft), stored at the Oklahoma Petroleum Information Center (OPIC), Geological Survey of Oklahoma, Norman. Bulk-rock samples for carbon isotope analysis were drilled from fresh rock surfaces in the field and from the core. Larger grains and calcite-filled fissures were avoided. Carbonate powders for isotope samples were reacted with 100% phosphoric acid at 70 °C using a Kiel IV carbonate device connected to a MAT 253 mass spectrometer. The CO_2 generated was used for analysing the carbon, calibrated by the Chinese national standard (GBW-04405) with a $\delta^{13}C$ value of 0.57 ± 0.03‰ (VPDB) during the analysis. The analytical precision is better than ±0.04‰ for $\delta^{13}C$. All the isotope analyses were carried out in the Stable Isotope Lab at the Nanjing Institute of Geology and Palaeontology, Chinese Academy of Sciences, China. All $\delta^{13}C_{carb}$ values are presented in Table 1 and have been cross-plotted with $\delta^{18}O_{carb}$ to analyse potential diagenetic alteration or overprint. Three large thin sections were produced at the Palaeontology Microfacies lab of Geozentrum Nordbayern in Erlangen from polished slabs; OKMC-1 = Cochrane Limestone at Holnam quarry, OKMC-2 = Keel Oolite at Holnam quarry, and OKMC-3 = Keel Oolite at Highway 77.

Results

Holnam quarry

The Holnam quarry in the Lawrence uplift is the type locality of the Keel Oolite (Amsden 1957, 1959). The section is situated in the highest quarried levels in the southeastern part of the quarry. This part of the quarry has been inactive for many years, and the sections are deteriorated and partly overgrown (Fig. 3A). Amsden & Barrick (1986) distinguished the basal Ideal Quarry Member overlain by the informal 'lower Keel oolite' and 'upper Keel oolite' at this locality. This stratigraphy corresponds to units 3–5 in Stanley (2001, fig. 18), who also introduced unit 6 for a thin interval of interbedded bioclastic grainstone and chert at the top of the formation. Amsden & Barrick (1986) noted a stylolite separating their lower and upper oolite facies (units 4–5), and this stylolite is at or near the horizontal fissure noted in the present study (used as reference level

Table 1. Sample levels (m) and $\delta^{13}C_{carb}$ and $\delta^{18}O_{carb}$ data from the three studied sections, Holnam quarry, Highway 77 road-cut and Sunray DX-Davis 1–5 drill core. All data are cross-plotted in Figure 9 herein, except H77-26, which we omitted due to its huge deviation from other data.

Holnam quarry				
Stratigraphic unit	**Sample**	**Metre**	**$\delta^{13}C_{carb}$**	**$\delta^{18}O_{carb}$**
Keel Oolite	HOQ-1	–0.8	1.15	–3.17
Keel Oolite	HOQ-2	–0.7	0.77	–3.20
Keel Oolite	HOQ-3	–0.6	2.10	–3.00
Keel Oolite	HOQ-4	–0.5	0.97	–3.99
Keel Oolite	HOQ-5	–0.4	0.65	–3.91
Keel Oolite	HOQ-6	–0.32	1.50	–3.42
Keel Oolite	HOQ-7	–0.25	0.82	–3.80
Keel Oolite	HOQ-8	–0.18	0.93	–3.74
Keel Oolite	HOQ-9	–0.1	1.15	–3.67
Keel Oolite	HOQ-25	+0.02	1.42	–3.60
Keel Oolite	HOQ-10	+0.1	1.39	–3.62
Keel Oolite	HOQ-11	+0.2	1.30	–3.72
Keel Oolite	HOQ-12	+0.3	1.24	–3.74
Keel Oolite	HOQ-13	+0.4	1.97	–3.44
Keel Oolite	HOQ-14	+0.5	1.56	–3.32
Keel Oolite	HOQ-15	+0.6	1.34	–3.57
Keel Oolite	HOQ-16	+0.7	0.83	–3.88
Keel Oolite	HOQ-17	+0.8	1.24	–3.88
Keel Oolite	HOQ-18	+0.9	1.38	–3.36
Keel Oolite	HOQ-19	+1.0	1.05	–4.15
Keel Oolite	HOQ-20	+1.1	1.27	–3.68
Keel Oolite	HOQ-21	+1.2	0.82	–3.74
Keel Oolite	HOQ-22	+1.3	1.28	–4.01
Cochrane Limestone	HOQ-23	lose slab	1.34	–3.75
Cochrane Limestone	HOQ-24	lose slab	1.11	–3.96

Highway 77				
Stratigraphic unit	**Sample**	**Metre**	**$\delta^{13}C_{carb}$**	**$\delta^{18}O_{carb}$**
Keel Oolite	H77-1	+0.02	–2.44	–3.32
Keel Oolite	H77-2	+0.06	–2.81	–3.46
Keel Oolite	H77-3	+0.1	–1.90	–3.17
Keel Oolite	H77-4	+0.16	–0.58	–2.72
Keel Oolite	H77-5	+0.2	–0.19	–3.51
Keel Oolite	H77-6	+0.26	–1.27	–3.37
Keel Oolite	H77-7	+0.30	–0.29	–3.41
Keel Oolite	H77-8	+0.35	–0.51	–3.26
Keel Oolite	H77-9	+0.40	–0.85	–3.18
Keel Oolite	H77-10	+0.45	–0.64	–3.23
Keel Oolite	H77-11	+0.51	–2.50	–3.53
Keel Oolite	H77-12	+0.57	–1.16	–3.10
Keel Oolite	H77-13	+0.61	0.06	–2.94
Keel Oolite	H77-14	+0.66	–1.49	–3.23
Keel Oolite	H77-15	+0.71	–1.78	–3.59
Keel Oolite	H77-16	+0.75	–0.95	–3.30
Keel Oolite	H77-17	+0.81	–0.80	–3.19
Keel Oolite	H77-18	+0.86	–1.32	–3.31
Keel Oolite	H77-19	+0.91	–0.50	–3.30
Keel Oolite	H77-20	+0.95	–0.19	–3.87
Cochrane Limestone	H77-21	+0.97	–5.01	–4.13
Cochrane Limestone	H77-22	+1.02	–2.45	–4.33
Cochrane Limestone	H77-23	+1.1	–3.35	–4.39
Cochrane Limestone	H77-24	+1.2	–2.71	–3.51
Cochrane Limestone	H77-25	+1.3	–2.00	–3.60
Cochrane Limestone	H77-26	+1.4	–9.68	–3.79
Cochrane Limestone	H77-27	+1.5	–4.99	–3.30
Cochrane Limestone	H77-28	+1.6	–5.84	–3.67
Cochrane Limestone	H77-29	+1.7	–2.22	–3.87
Cochrane Limestone	H77-30	+1.8	–2.24	–3.56
Cochrane Limestone	H77-31	+1.9	–4.11	–3.74
Cochrane Limestone	H77-32	+2.07	–1.13	–3.85
Cochrane Limestone	H77-33	+2.15	–1.13	–3.96
Cochrane Limestone	H77-34	+2.22	–0.82	–3.86
Cochrane Limestone	H77-35	+2.3	–0.74	–3.89
Cochrane Limestone	H77-36	+2.4	–0.78	–4.06

Highway 77, continued				
Stratigraphic unit	**Sample**	**Metre**	**$\delta^{13}C_{carb}$**	**$\delta^{18}O_{carb}$**
Cochrane Limestone	H77-37	+2.5	–1.68	–4.05
Cochrane Limestone	H77-38	+2.6	–0.44	–3.58
Cochrane Limestone	H77-39	+2.72	0.04	–3.59
Clarita Formation, Fitzh.Mb.	H77-40	+3.0	2.91	–2.96
Clarita Formation, Fitzh.Mb.	H77-41	+3.1	0.10	–4.78
Clarita Formation, Fitzh.Mb.	H77-42	+3.19	3.52	–2.43
Clarita Formation, Fitzh.Mb.	H77-43	+3.3	3.62	–2.55
Clarita Formation, Fitzh.Mb.	H77-44	+3.4	0.54	–4.54
Clarita Formation, Fitzh.Mb.	H77-45	+3.5	2.97	–2.93
Clarita Formation, Fitzh.Mb.	H77-46	+3.6	1.76	–4.16
Clarita Formation, Fitzh.Mb.	H77-47	+3.7	2.88	–3.12
Clarita Formation, Fitzh.Mb.	H77-48	+3.8	1.69	–4.17
Clarita Formation, Fitzh.Mb.	H77-49	+3.9	2.78	–3.15
Clarita Formation, Fitzh.Mb.	H77-50	+4.0	–1.93	–6.45
Clarita Formation, Fitzh.Mb.	H77-51	+4.1	–1.39	–6.59
Clarita Formation, Fitzh.Mb.	H77-52	+4.3	2.22	–3.21
Clarita Formation, Fitzh.Mb.	H77-53	+4.5	2.52	–2.88
Clarita Formation, Fitzh.Mb.	H77-54	+4.7	2.04	–3.15
Clarita Formation, Fitzh.Mb.	H77-55	+4.9	3.04	–2.55
Clarita Formation, Fitzh.Mb.	H77-56	+5.1	1.78	–3.39
Clarita Formation, Fitzh.Mb.	H77-57	+5.3	1.62	–3.24
Clarita Formation, Fitzh.Mb.	H77-58	+5.5	2.10	–3.16
Clarita Formation, Fitzh.Mb.	H77-59	+5.7	1.97	–3.08
Clarita Formation, Fitzh.Mb.	H77-60	+5.9	1.45	–3.44
Clarita Formation, Fitzh.Mb.	H77-61	+6.1	1.38	–3.38
Clarita Formation, Fitzh.Mb.	H77-62	+6.3	–2.12	–6.64
Clarita Formation, Fitzh.Mb.	H77-63	+6.5	0.90	–4.25
Clarita Formation, Fitzh.Mb.	H77-64	+6.73	1.08	–4.30
Clarita Formation, Fitzh.Mb.	H77-65	+6.85	0.33	–4.82
Henryhouse Formation	H77-66	+6.93	0.40	–3.54
Henryhouse Formation	H77-67	+7.2	1.06	–3.89
Henryhouse Formation	H77-68	+7.4	0.21	–3.35
Henryhouse Formation	H77-69	+7.6	0.077	–2.52
Henryhouse Formation	H77-70	+7.8	0.224	–2.72
Henryhouse Formation	H77-71	+8.0	0.32	–2.97
Henryhouse Formation	H77-72	+8.2	–0.198	–4.36
Henryhouse Formation	H77-73	+8.4	–0.102	–3.98
Henryhouse Formation	H77-74	+8.6	–3.181	–3.59
Henryhouse Formation	H77-75	+8.8	–0.86	–2.92
Henryhouse Formation	H77-76	+9.55	0.489	–1.90
Henryhouse Formation	H77-77	+9.65	0.871	–0.76

Sunray DX-Davis 1-5				
Stratigraphic unit	**Sample**	**Metre**	**$\delta^{13}C_{carb}$**	**$\delta^{18}O_{carb}$**
Cochrane Limestone	SDX-1	+3.5	–1.03	–2.85
Cochrane Limestone	SDX-2	+3.0	–0.56	–3.17
Cochrane Limestone	SDX-3	+2.6	–2.37	–5.03
Cochrane Limestone	SDX-4	+2.2	–1.01	–5.13
Cochrane Limestone	SDX-5	+1.55	–1.91	–5.71
Cochrane Limestone	SDX-6	+1.10	–1.89	–5.81
Cochrane Limestone	SDX-7	+1.05	–2.14	–5.78
Cochrane Limestone	SDX-8	+0.7	–0.10	–4.92
Cochrane Limestone	SDX-9	+0.4	0.01	–5.08
Cochrane Limestone	SDX-10	+0.35	0.11	–4.43
Keel Oolite	SDX-11	–0.15	0.28	–4.76
Keel Oolite	SDX-12	–0.7	0.73	–4.51
Keel Oolite	SDX-13	–1.0	0.59	–4.70
Keel Oolite	SDX-14	–1.3	0.85	–4.67
Keel Oolite	SDX-15	–1.5	0.19	–4.85
Keel Oolite	SDX-16	–1.8	1.17	–4.25
Keel Oolite	SDX-17	–2.1	–0.38	–5.05
Keel Oolite	SDX-18	–2.4	1.22	–3.75
Keel Oolite	SDX-19	–2.8	0.55	–3.89
Keel Oolite	SDX-20	–3.1	–0.83	–4.86

herein). Above this level, in their 'upper Keel oolite', they identified an irregularly distributed skeletal packstone with *Brevilamnulella* sp. and the horn coral *Streptelasma* sp. (the so-called '*Brevilamnulella*-coral beds' of Amsden & Barrick 1986). The ooids in this interval (unit 5) are in some levels unusually large (~ 3.5 mm = pisolites) and enclosed in a coarsely crystalline cement (Fig. 3B). The larger ooids tend to have a distinct, finely concentric structure with very small nucleus to cortex ratio, while the smaller fraction are generally of radial type and with a larger nucleus to cortex ratio. The nuclei are, in most cases, unidentifiable for the large fraction and a crinoidal plate for the small fraction (Fig. 3C, D). This upper oolite (unit 5) is overlain by a thin layer of chert (unit 6), in turn overlain by the Cochrane Limestone, although the contact could not be seen due to scree in the section. The lithology of the lower portion of the Cochrane is typically a glauconitic, well-sorted crinoidal packstone to grainstone (Fig. 3E, F). Abundant loose material of this lithology, yielding distinct subvertical solution pipes filled with brown-colored matrix, was found on the quarry ledge that coincides with the Keel–Cochrane boundary, but no *in situ* findings, and thus the stratigraphic position or age for this apparent karst horizon was not possible to define in the field.

The carbon isotope samples reported herein were drilled from the same *ca.* 2-m-high ledge section that was studied by Amsden & Barrick (1986, p. 8), exposing the full thickness of the Keel Oolite (Fig. 3A). Carbon isotope

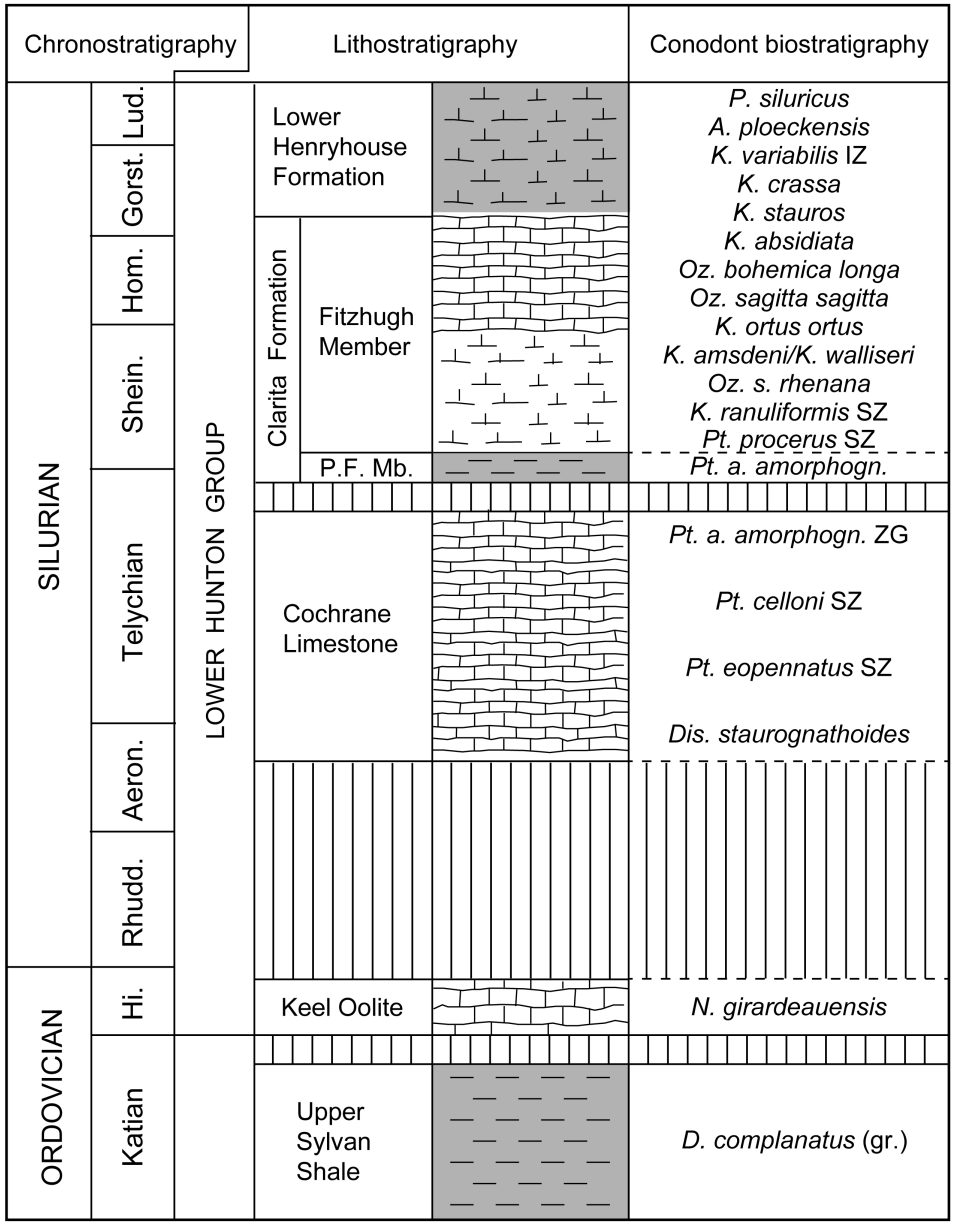

Figure 2. Chronostratigraphy of the Ordovician–Silurian boundary interval and the Lower Hunton Group in Oklahoma, and thus not scaling the true thickness of the lithostratigraphic units. The figure is based on the combined information from previously published conodont biostratigraphy, from several different localities and areas of Oklahoma (Barrick & Klapper 1976, Amsden *et al.* 1980, Barrick *in* Amsden & Barrick 1986, Barrick *et al.* 2010a, and references therein). The biostratigraphy varies substantially locally, and the studied section in the Arbuckles shows several additional hiatuses.

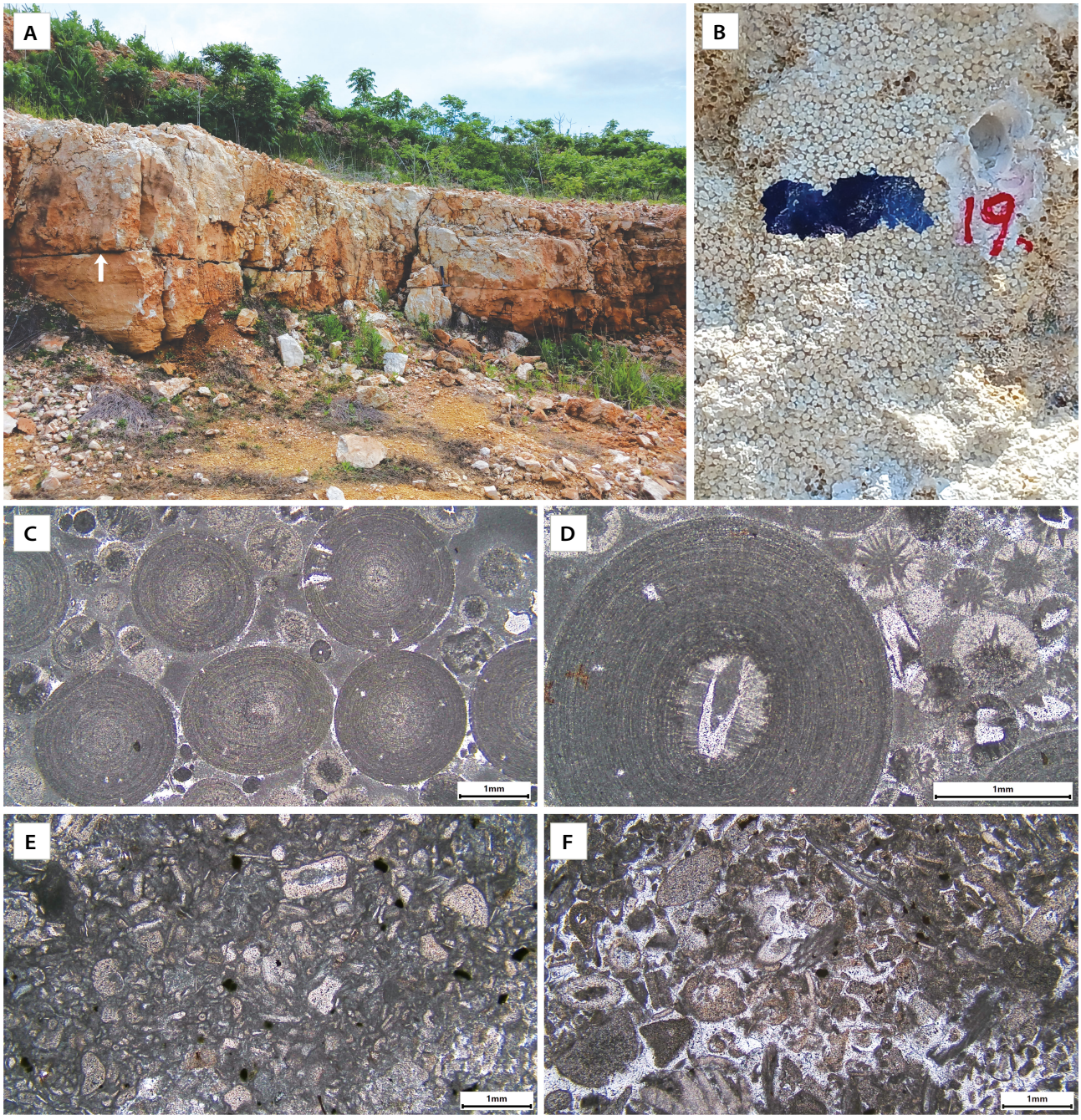

Figure 3. Photographs showing section and rock samples at the Holnam quarry, Pontotoc County. • A – the section studied herein is the same section as described by Amsden & Barrick (1986, p. 8). White arrow marks an open cleft in the section, used as reference level herein. This level corresponds closely to the boundary between the 'lower' and 'upper Keel oolite' of Amsden & Barrick (1986, fig. 15) and units 4 and 5 of Stanley (2001, fig. 18). • B – close up of the higher portions of the section (unit 5) with abundant, large, and slightly over-packed ooids at the level of carbon isotope sample no. 19 (in Fig. 4). • C – thin section photograph showing bimodally sorted oolite from unit 5 (sample OKMC-2). • D – detail of large concentric ooid from unit 5 (sample OKMC-2). • E – crinoidal packstone microfacies in the basal Cochrane Limestone (sample OKMC-1). • F – crinoidal grainstone microfacies of the basal Cochrane Limestone (sample OKMC-1).

values of the Keel Oolite show no clear stratigraphic trend and scatter with small variation around an almost vertical trendline, rising from +1.2–1.3‰. The two highest $\delta^{13}C$ values reach +1.97‰ and +2.10‰. Additional $\delta^{13}C$ values sampled from the Ideal Quarry Member and the 'lower Keel oolite' in the same part of the quarry by Jim Barrick (unpublished), reach +2.22‰ and +2.44‰, respectively. Two isotope samples drilled from the pack-grainstone between two karst solution pipes in the basal Cochrane show similar $\delta^{13}C$ values near above +1‰ (Fig. 4).

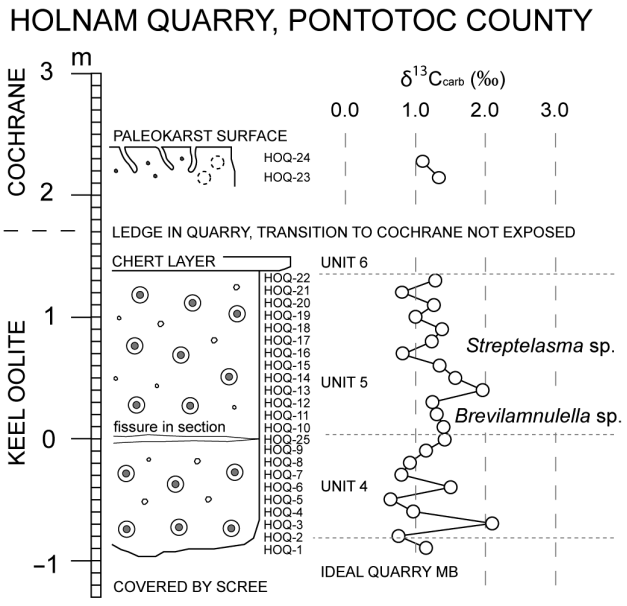

Figure 4. Lithologic log of the Keel Oolite at Holnam quarry with carbon isotope stratigraphy. Unit 4–6 adapted after Stanley (2001, fig. 18).

Highway 77 road-cut

This locality constitutes a *ca.* 45-m-thick succession of strata of Late Ordovician through Early Devonian age (Fig. 5A, B). The strata are overturned due to the local Washita fault system and are dipping at *ca.* 80° to the southwest and striking N62°W (see Stanley 2001, stop 8, pp. 59–64 for a detailed description of the entire succession). The part of the section studied herein encompasses the Keel Oolite (0.96 m), Cochrane Limestone (1.8 m), Clarita Formation (4.15 m, of which the Prices Fall Member is *ca.* 0.25 m and the Fitzhugh Member is *ca.* 3.9 m), and the lowermost ca 3 m of the Henryhouse Formation (interpreted as corresponding to units 1/2 and 3 of Barrick *et al*. 2010a, pp. 57, 58) (Fig. 5B–E). The Keel Oolite channels into the Sylvan Shale and the thickness of the oolite therefore varies slightly laterally. The microfacies of the oolite include packstone and grainstone with thin-bedded alternations between these. The oolite includes abundant sand-sized, micritic, coated grains that at least partly have a microbial origin and therefore are micro-oncoids rather than ooids (Fig. 5F). Crinoidal fragments constitute the most common bioclasts (Fig. 5G). The top of the Keel is a clear-cut erosional surface overlain by the Cochrane Limestone (Fig. 5C). The Cochrane Limestone constitutes a bioclastic, mainly crinoidal, packstone and grainstone, with very little insoluble material (normally < 5%; Amsden 1959) and with common glauconite. In the Highway 77 road-cut the glauconite appears more common in the upper part of the unit. The top of the Cochrane Limestone is sharp and planar and is based on convincing regional outcrop features interpreted as an unconformity (Amsden 1959, pp. 50, 60; Amsden *et al.* 1980). The *ca.* 0.25-m-thick shale that overlies this unconformity constitutes the Prices Falls Member of the Clarita Formation (Fig. 5D). Due to its soft character, it is weathered and deeply recessed in the section. The overlying Fitzhugh Member of the Clarita Formation is a calcareous mudstone in which the middle and upper parts are more calcareous than the lower parts (Fig. 5E). It should be noted that the contact between the Clarita and overlying Henryhouse formations may be difficult to point out precisely. This boundary is locally developed as an unconformity, and the Henryhouse Formation is clearly more argillaceous than the underlying Clarita Formation. In some areas, however, the uppermost Clarita is also more argillaceous and any unconformity is less conspicuous or absent, for example, in the Murray County south of Davis, where the Highway 77 road-cut is located (Amsden 1959, p. 53). In the Highway 77 road-cut we have put the boundary 3.9 m above the base of the Fitzhugh Member and between isotope samples H77-65 and H77-66, as the Clarita facies becomes clearly more argillaceous at that level (Fig. 7).

Carbon isotope values of the Keel Oolite are moderately negative and show a positive trendline from *ca.* −1.6‰ to −0.6‰ through the section (Fig. 6). A few observations may be of significance: The two lowest samples, near the base of the unit, also record the two lowest values and are followed by a steady increase in the lowermost 0.2 m of the unit. Thereafter, the $\delta^{13}C$ values scatter broadly around the trend line through the remainder of the unit, mostly in the positive (higher) values. The two uppermost $\delta^{13}C$ values are followed by a negative shift of 2–3‰ in the basal Cochrane Limestone. This shift provides chemostratigraphic support for the hiatus previously established by biostratigraphy and marked by a clear-cut unconformity at this level. The $\delta^{13}C$ values of the lowermost meter of the overlying Cochrane Limestone shows a strong scatter of values, between *ca.* −6‰ and −2‰. In the uppermost *ca.* 0.8 m the $\delta^{13}C$ values concentrate between −1‰ and 0‰. The overall trend line through the Cochrane Limestone shows a steady increase in $\delta^{13}C$ values with the most positive value of 0‰ at the very top of the formation. This upper boundary is based on the combined information from biostratigraphy, sedimentology and carbon isotope stratigraphy, an unconformity associated with some degree of hiatus. No $\delta^{13}C$ analyses were conducted on the overlying, shaly, Prices Falls Member of the Clarita Formation. The lowermost part of the Fitzhugh Member of that same formation shows consistently higher $\delta^{13}C$ values compared to the underlying Cochrane Limestone, with upwards reduced scatter of data. The basal part of the slightly more calcareous upper portion of the Fitzhugh Member shows a substantial drop in two $\delta^{13}C$ values possibly signifying a disconformity

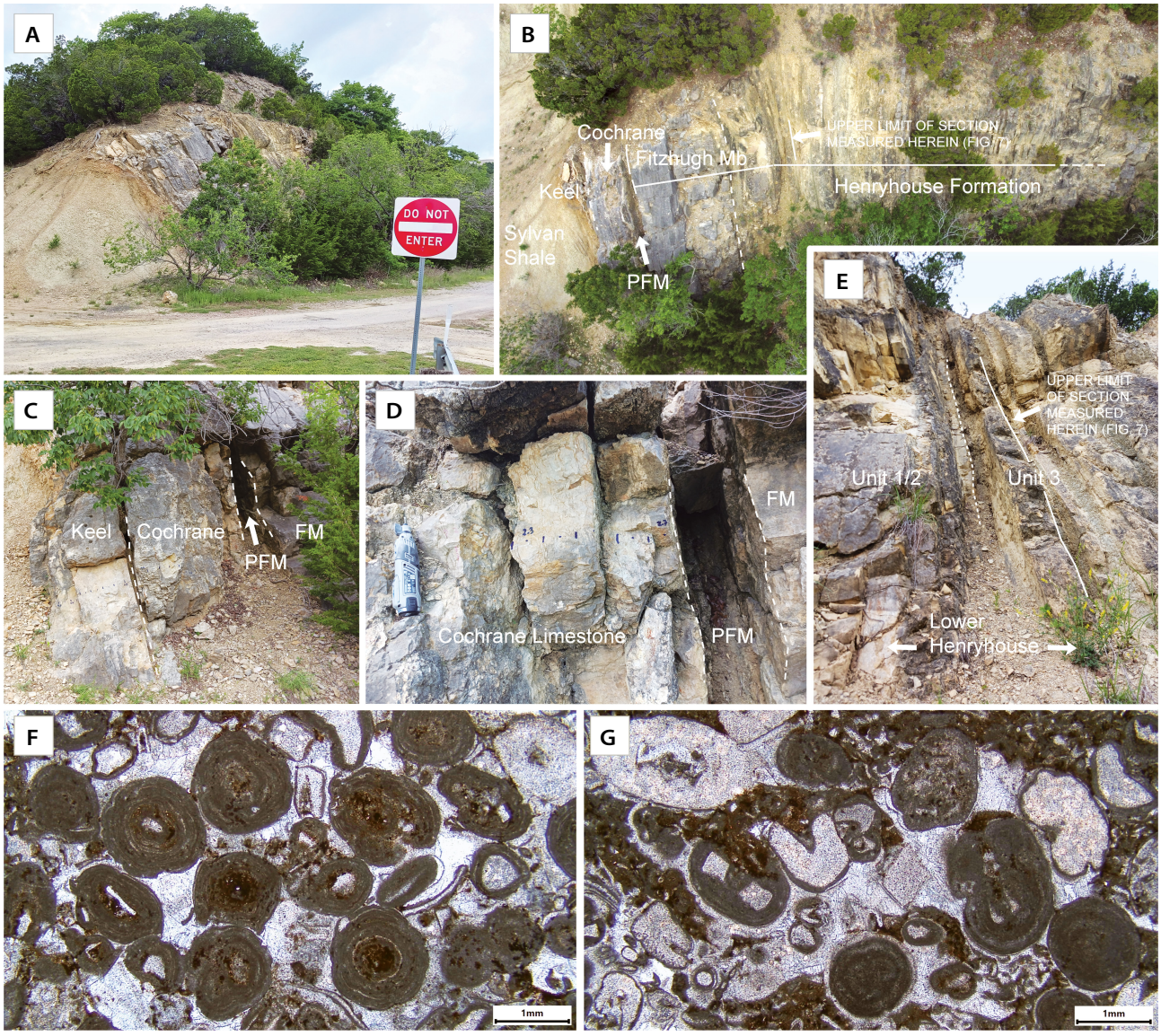

Figure 5. Photographs showing Highway 77 road-cut south of Davis. The lower (southernmost) portions, which exhibit the Ordovician–Silurian transition, were sampled for this study. • A – view of locality from Highway 77 with the weathered Sylvan Shale to the left. • B – drone view of the section showing overall stratigraphy. The interval from the base of the Keel Oolite to the basal Henryhouse Formation was sampled for this study. • C – Keel Oolite and Cochrane Limestone are separated by a clear-cut unconformity (white dashed line). PFM = Prices Falls Member of the Clarita Formation. • D – lower portions of the Cochrane Limestone overlain by the Prices Falls Member (PFM) and the Fitzhugh Member (FM) of the Clarita Formation. • E – top of the studied section at the boundary between the Clarita Formation and the Henryhouse Formation. The stratigraphic thickness from the base of the Keel Oolite to the top of the Clarita Formation is *ca.* 6.9 m. • F – coated grains in the Keel Oolite (grainstone) are dominantly micritic with irregular cortex lamination, suggesting a microbial origin. • G – bioclasts in the Keel Oolite are dominantly crinoidal debris.

at this level, although this was not obvious in the field. The remainder of the Fitzhugh Member shows a steady decline from $\delta^{13}C$ values between 2–3‰ near the base to around 0‰ near the top (except two single and separated values that are more negative). $\delta^{13}C$ values then increase again in the most basal part of the overlying Henryhouse Formation.

Biostratigraphic assessment of the 77 road-cut. – To support our $\delta^{13}C$ record and to understand its value for correlation, we herein include a summary of key biostratigraphic data previously published from the upper Sylvan Shale through lower Henryhouse Formation in the area, and from the Highway 77 road-cut. The upper Sylvan Shale in the Arbuckle Mountains falls within the *Dicellograptus complanatus* graptolite Zone (Goldman & Bergström 1979), whereas the Keel Oolite belongs in the *Noixodontus girardeauensis* conodont Zone, which internationally corresponds to the late *Metabolograptus persculptus* graptolite Zone. It is noted here that none of

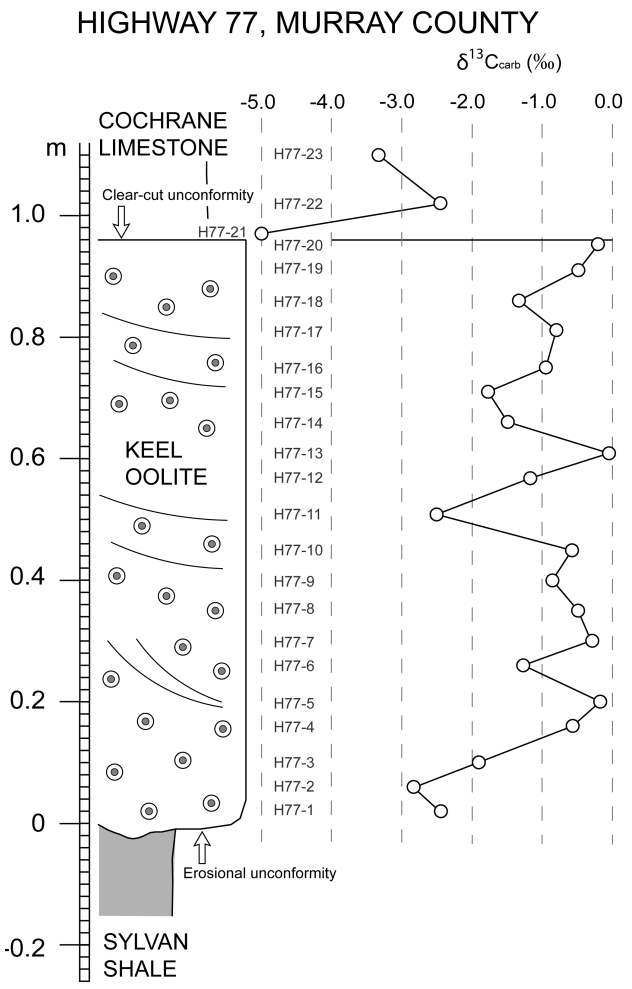

Figure 6. Carbon isotope stratigraphy of the Keel Oolite at the Highway 77 road-cut. Note strongly negative isotope values.

these findings derive immediately from the Highway 77 section, but they are locally derived data and it is therefore likely that at least one and a half graptolite zones are missing in the contact between these consecutive units.

Distomodus staurognathoides, which would indicate either uppermost Aeronian or lowermost Telychian, have been recovered from the lower Cochrane Limestone in the Arbuckles but not from the Highway 77 section (*cf.* Fig. 7). This taxon is concurrent with the falling limb of the Late Aeronian Carbon Isotope Excursion (LACIE) and the onset of the Valgu Event in other regions (Munnecke & Männik 2009). Hence, although we cannot be sure it is the lower Cochrane that is outcropping at Highway 77, it is plausible that the distinct lowering of $\delta^{13}C$ values seen in the lowermost *ca.* 0.6 m of this limestone represents the LACIE. Hence, based on the available data, the Rhuddanian and most of the Aeronian are missing at the top Keel unconformity at the Highway 77 road-cut.

It is possible that the upper *Dis. staurognathoides* Zone is missing. Based on comparison with published records of the Valgu Event, even where it is condensed, we can assume, however, that the *Pt. eopennatus* and *Pt. celloni* zones should at least partly be present at this locality. We suggest that the distinctly rising $\delta^{13}C$ values in the upper Cochrane Limestone represent parts of the Valgu Carbon Isotope Excursion (Valgu CIE), an interval that based on conodonts includes the Valgu Bioevent (Männik 2007b).

The conodont biostratigraphy of the overlying Clarita and Henryhouse formations has been studied by Barrick & Klapper (1976) and by Barrick *et al*. (2010a, b), respectively. A single specimen of *Pterospathodus amorphognathoides amorphognathoides*, and several other taxa typical of this zone, were found in the Prices Falls Member by Barrick & Klapper (1976, their sample 11, tab. 1). A second element of *Pt. a. amorphognathoides* was found immediately above the shale, in sample 12 in the lowermost part of the overlying Fitzhugh Member. This sample also included conodonts diagnostic of the *Pt. celloni* Zone, but also conodonts ranging higher up (Barrick & Klapper, 1976, p. 64). Based on these findings, we select the base of the Prices Falls Member as the base of the *Pt. a. amorphognathoides* Zone. The thinness of this member, its anomalous facies (shale), and the distinct offsets in our isotope record at its lower and upper boundaries suggest that the corresponding conodont zone, which extends into the Sheinwoodian (Jeppsson *et al*. 2006), is not completely preserved at this locality.

The overlying Fitzhugh Member constitutes bioclastic wackestone that contains faunas of the *K. ranuliformis*, *K. amsdeni*, *K. stauros* and the *K. crassa* zones (Barrick & Klapper 1976). The first two zones have more recently been lumped and included in the *K. ranuliformis* Zone (Simpson *et al*. 2021). We note here, however, that Silurian conodont zonation has changed in detail several times over the last few decades, depending on the philosophy of conodont workers and between different countries and continents. We argue that, for local correlations, it is useful to keep the *K. amsdeni* Zone, because it has been clearly shown in different papers by Jim Barrick and co-workers

Figure 7. Lithologic log and carbon isotope stratigraphy of the Highway 77 road-cut. Major hiatuses are bracketing the Keel Oolite, of which the O/S-boundary unconformity spans the latest Hirnantian through Rhuddanian and most of the Aeronian. Additional unconformities are associated with both the Cochrane and Clarita formations, although their biostratigraphic significance is difficult to assess (see text). The white squares with numbers in the Clarita Formation refer to the approximate sample levels of Barrick & Klapper (1976, p. 63, tab. 1) and bold conodont names indicate actual zones present at this locality, with adhering sample number within brackets. Biostratigraphic data, unit subdivision, and selected sample numbers (301, 303, 303A) in the lower Henryhouse Formation derives from Barrick *et al*. (2010a). The conodont names in brackets refer to the general conodont

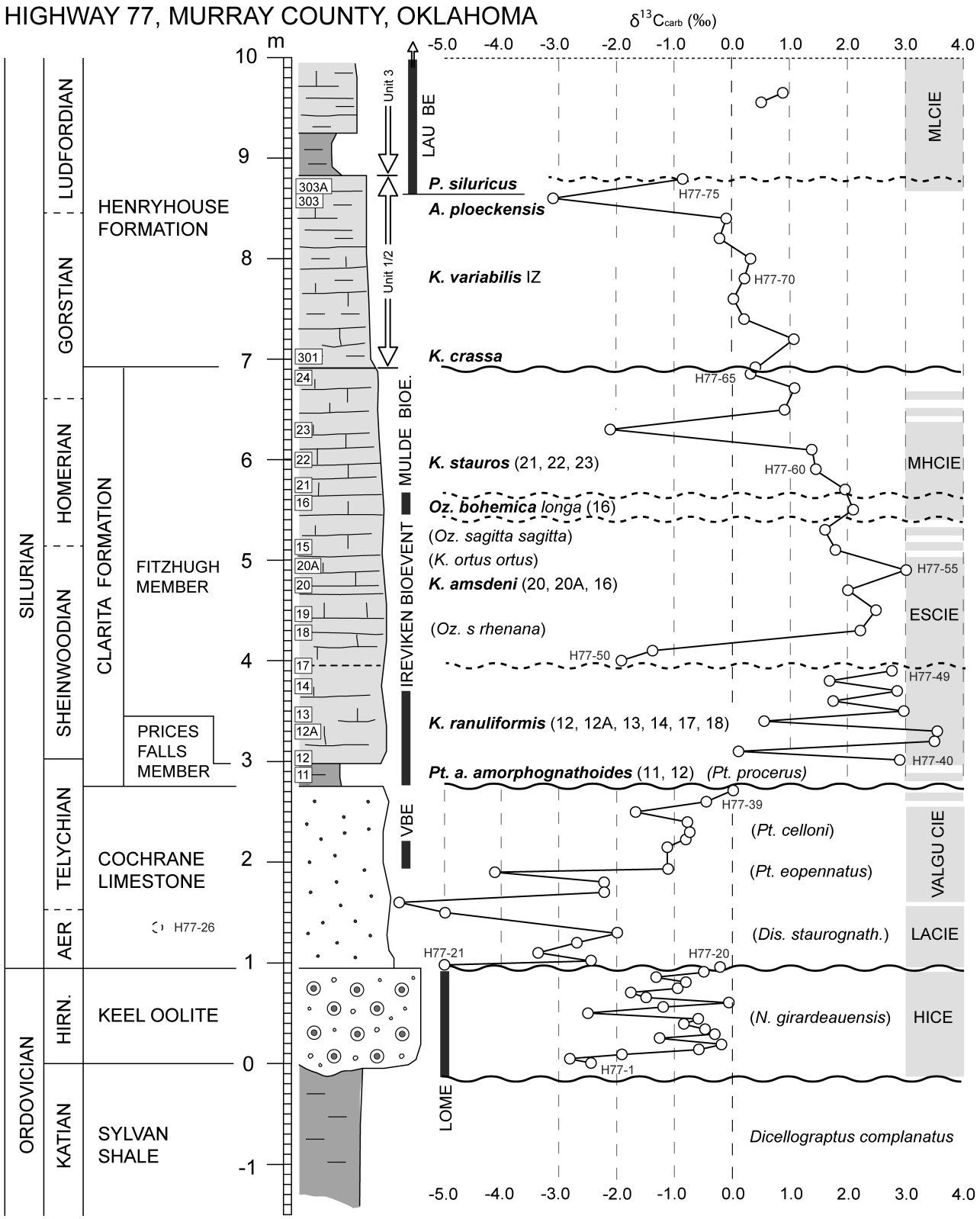

biostratigraphy with zones that could be present based on studies of other localities in the Arbuckle area by various authors and are only included as a general support to the stratigraphy. Conodont biostratigraphy, however, undoubtedly shows that the *K. absidata* zone is missing and likely cut out at an unconformity. The presence of some of the widely known carbon isotope excursions can be inferred but it should be stressed that some of these are highly tentative as none of them are fully preserved. The black vertical bars indicate the tentative position of bioevents.

that it has value for global correlation. The *K. stauros* and *K. crassa* zones are today often lumped into an extended *K. crassa* Zone (*sensu* Corradini *et al*. 2015). Also, in this case, however, we keep these two zones separated for reliable and more detailed correlations in this part of southern Laurentia.

The generally high $\delta^{13}C$ values between the first appearance datum (FAD) of *Pt. a. amorphognathoides* in sample 11 and a level just below the FAD of *Ozarkodina bohemica longa* in sample 16 are herein interpreted as part of the Early Sheinwoodian Carbon Isotope Excursion (ESCIE; frequently termed the "Ireviken excursion"), which is then restricted to the lowermost *ca.* 2.4 m of the Fitzhugh Member. The major offset in $\delta^{13}C$ values at +4 m in Figure 7 may thus indicate an intra-ESCIE unconformity. The presence of *Oz. b. longa* in sample 16 is firm evidence that these strata belong within the stratigraphic range of the Mulde Bioevent and the Mid Homerian Carbon Isotope Excursion (MHICE; *cf*. Calner & Jeppsson 2003, Calner *et al*. 2006, Barrick *et al*. 2009, Biebesheimer *et al.* 2021). It is not possible to state which part of the MHICE is present in the Highway 77 record, but it presumably does not extend above the unconformity below the *K. crassa* Zone. The *K. crassa* Zone is followed by the *K. variabilis* Interval Zone, which represents the only interval zone in the studied succession, and which is defined by the LAD of *K. crassa* and the FAD of *A. ploeckensis*. The corresponding succession shows only minor variation in $\delta^{13}C$ values, until a substantial drop within the *A. ploeckensis* Zone (only one sample though). The *A. ploeckensis* Zone is documented in sample level 303 of Barrick *et al*. (2010a; Fig. 7), and is overlain by strata with *P. siluricus,* indicating that datum point 1 of the Lau Bioevent should be placed at this level. Above this level our three remaining carbon isotope samples reflect the onset of the strong positive Mid Ludfordian Carbon Isotope Excursion (MLCIE) in the lower Henryhouse (Fig. 7), corroborating the results of Barrick *et al.* (2010a). The *Oz. snajdri* Zone, the next younger zone described by Barrick *et al*. (1990, pp. 55–62; 2010a) is much higher up in the Henryhouse and there is no indication yet that the "Icriodontid" interval or zone known from Baltica is present between the *P. siluricu*s Zone and the *Oz. snajdri* Zone.

Sunray DX-Davis 1–5 drill core

The studied part of the Sunray drill core includes the Keel–Cochrane transition. The Keel Oolite is at least 3.1 m thick but may be thicker as no core below core box 8 is available for study. The variably oolitic grainstone is partly laminated and partly has a mottled texture. Contact with the overlying Cochrane is not preserved in any

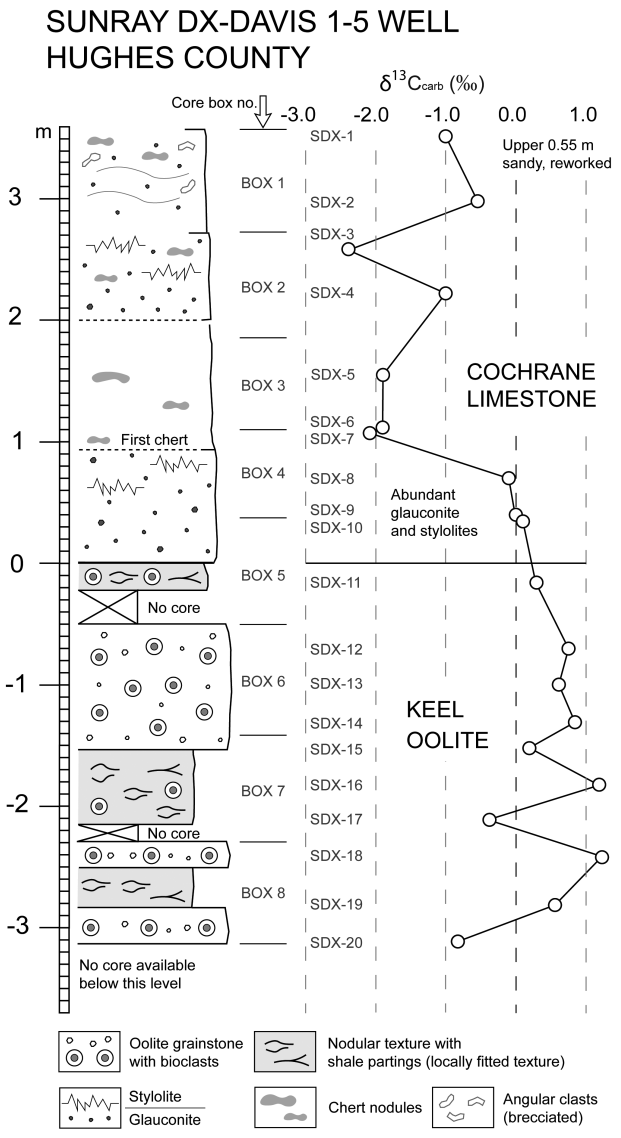

Figure 8. Lithologic log and carbon isotope stratigraphy of the Sunray DX-Davis 1–5 drill core. Notably, the carbon isotope stratigraphy does not show any offset across the boundary between the Keel Oolite and the Cochrane Limestone, which may indicate that a hiatus is lacking in this area, which is further to the northeast of the central Arbuckles.

continuous core piece and the sedimentary features and characteristics of this transition are therefore not known. There is a distinct colour contrast, however, between the Keel and the Cochrane, the former having a brownish tint, likely from hydrocarbons.

Carbon isotope values of the Keel Oolite scatter along a weakly positive trend line from *ca.* −1.7‰ to −0.5‰. Of particular interest is the lack of any deflection in the $\delta^{13}C$ values across the Keel–Cochrane boundary. It could indicate that this transition is conformable in the core, but we consider it unlikely as this section is relatively close to several others where the Keel–Cochrane boundary is associated with a hiatus spanning 4–5 million years.

Discussion

We have cross plotted all carbon and oxygen data to understand the degree of co-variance and diagenetic alteration to the studied sections (Fig. 9). Correlations between C and O values are low overall with R^2 values normally well below 0.5, and thus comparable to many other Ordovician marine limestone successions that are assumed to reflect a largely primary isotopic signal, *e.g.* Lindskog *et al*. (2019), Yang *et al*. (2020), Gul *et al.* (2021). The exception is the Clarita Formation, which stands out with a high $R^2 = 0.94$, suggesting more extensive alteration. The Keel Oolite is compared separately for correlation potential purposes, and because it represents a very specific and unusual, shallow marine depositional system and time-specific facies. Our data from the oolite show a range of correlations from $R^2 = 0.04$ at the Highway 77 road-cut, to $R^2 = 0.29$ at Holnam quarry, and to $R^2 = 0.49$ in the Sunray DX-Davis 1–5 core (Fig. 9A). Thus, the $\delta^{13}C$ signal is arguably isotopically pristine at the Highway 77 road-cut, whereas weak to moderate diagenetic modification is likely for the oolites at Holnam quarry and in the Sunray core successions. In sections around the World, the HICE ideally starts at baseline values near 0‰ or +1‰ and rises to a peak or extended plateau ranging between 4‰ to 6‰ before the value decreases again to near the original baseline (Brenchley *et al.* 2003; Bergström *et al.* 2012, 2014; Bergström & Goldman 2019). In strata representing shallow-marine environments, the rising and falling limbs of the HICE often occur over a very thin succession of strata or are cut-out, leaving near-horizontal or horizontal lines in the $\delta^{13}C$ record. The reason is normally the lowstand erosion following forced (glacio-eustatic) regression (rising limb),

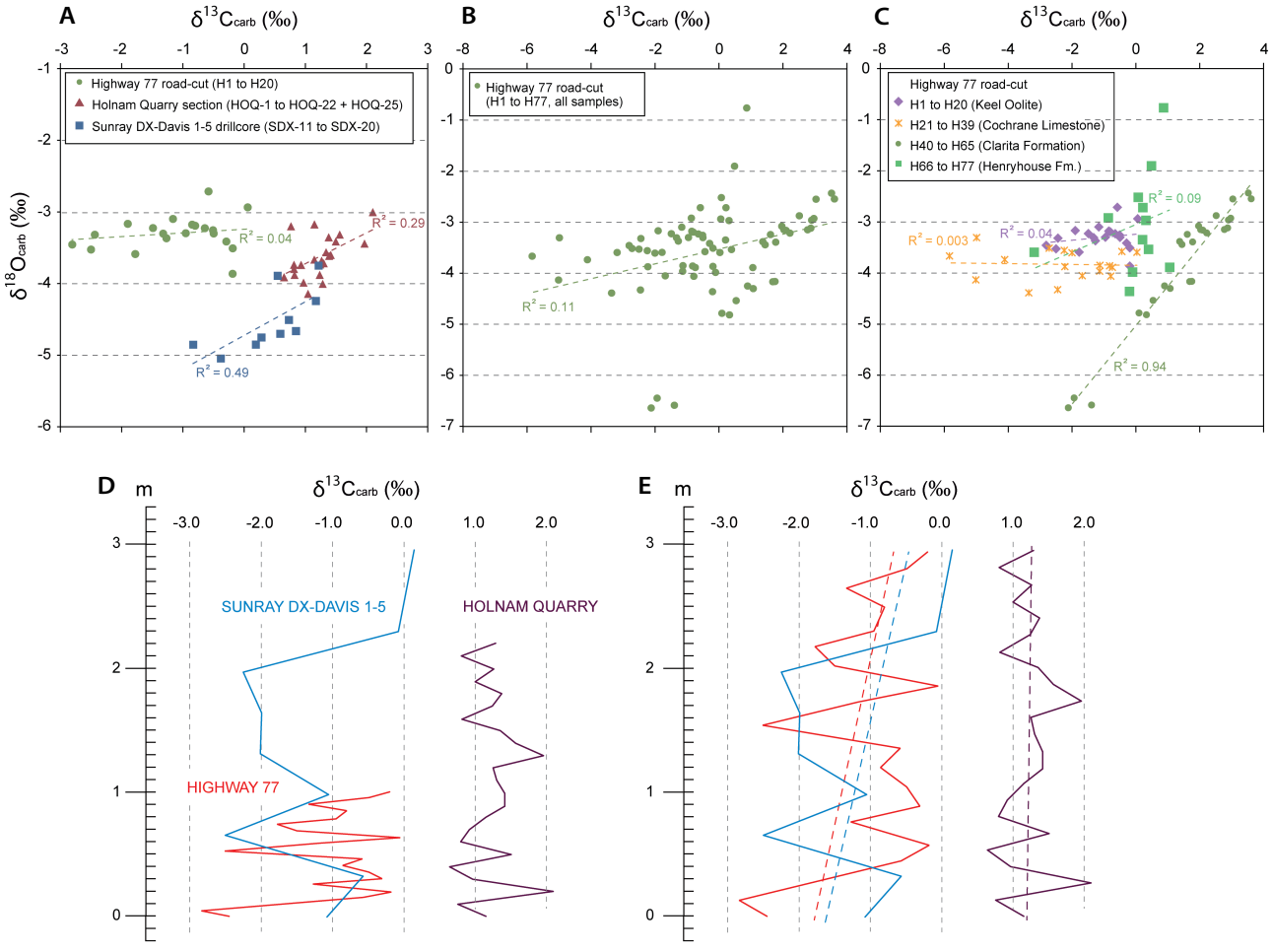

Figure 9. Cross plots of carbon and oxygen stable isotopes. See main text for discussion. • A – Keel Oolite at the three studied localities. • B – highway 77 road-cut, all stable isotope data summarised. • C – highway 77 road-cut with a cross plot of stable isotope data separated per lithological unit. • D – Keel Oolite $\delta^{13}C$ values plotted against thickness for comparison. • E – Keel Oolite $\delta^{13}C$ values plotted assuming the oolite represents the same time interval for all localities, for comparison of trend lines (dashed lines), which are positive (Highway 77 and Sunray drill core) or without any clear trend (Holnam quarry).

but may also be due to extreme condensation during post-glacial transgression (falling limb). Many Hirnantian stratal packages therefore show only parts of the peak and plateau interval of the HICE. Within this interval, the $\delta^{13}C$ values often show a weak trend of increasingly positive $\delta^{13}C$ values up-section. Good examples of this common and distinct trend are documented from the Blackstone River section in the Yukon Territory (LaPorte *et al.* 2009), in the Laframboise Member of the Ellis Bay Formation in western Anticosti (Bergström *et al*. 2014), and from the Girardeau Formation in southernmost Illinois (McAdams *et al*. 2018). We infer that this trend is what we also see in the herein studied sections, since, at all three localities the presumably intact trendline is vertical or slightly increasing towards higher $\delta^{13}C$ values (Fig. 9D, E). No rising limb or falling limb has been preserved, which is corroborated by sedimentary evidence for erosional unconformities. It is notable, especially in light of the low R^2 values that carbon data of the HICE are shifted towards negative values in all studied sections and especially in the Highway 77 and Sunray core sections. Diagenetic alteration that would shift the values in this direction includes interaction with oxidation of organic matter during early diagenesis or meteoric diagenesis and recrystallisation. The latter appears most plausible in these sections as they are bracketed by unconformities that assume a substantial degree of subaerial exposure. It is noted here that the carbon isotope stratigraphy and brachiopod fauna of the Keel Oolite is partly in conflict in terms of the age of the strata: Our isotope data imply that only parts of the peak and plateau of the HICE are preserved – although there is some uncertainty about the Holnam quarry, from where at least four $\delta^{13}C$ values are near or above 2‰ in the lowermost part of the section (including the unpublished data of Jim Barrick). The $\delta^{13}C$ values following above are consistently lower and this overall decrease may signal that the strata formed during the time corresponding to the falling limb of HICE. More expanded sections need to be studied to settle this and overall, our data broadly fit with the $\delta^{13}C$ trend documented from the middle-upper *M. extraordinarius* through earliest *M. persculptus* graptolite zones (*e.g*. Bergström *et al.* 2014), suggesting a middle Hirnantian age. The presence of brachiopods of the Edgewood–Cathay Fauna in the same strata (e.g. *Brevilamnulella*) on the other hand suggests a latest Hirnantian age associated with the upper *M. persculptus* graptolite Zone (*cf.* Rong *et al*. 2020).

For the Silurian part of the section at Highway 77 our data show low overall co-variance, except for the Clarita Formation (Fig. 9B, C). The only previous studies on $\delta^{13}C$ stratigraphy of the basal Silurian in the Arbuckle Mountains are those of Saltzman (2001) and Barrick *et al*. (2010a, b). Saltzman (2001) described a $\delta^{13}C$ rise of 6‰ from the middle part of the Cochrane Limestone (−2‰) to the lower part of the Fitzhugh Member of the Clarita Formation (+4‰), followed by a drop back to the interval between −1‰ to 0‰ at the top of the Fitzhugh Member (Saltzman 2001, fig. 2). Our data confirms the general isotopic trend reported by that study, with a general rise, peak and fall. In addition, our study adds substantially increased stratigraphic detail, which shows that this record is interrupted by several unconformities. Barrick *et al*. (2010a, b) analysed the carbon isotope stratigraphy of the lower Henryhouse Formation and documented the onset of the Lau Event. Our three topmost carbon isotope samples were taken in strata with *P. siluricus* and they indicate a rise, and therefore corroborates the results of Barrick *et al*. (2010a, b).

Conclusions

Our study reveals challenges with using high-resolution carbon isotope stratigraphy for even local correlation of the Hirnantian oolites in the Arbuckle Mountains, but it serves well to reveal hiatuses and incompleteness in the stratigraphic succession. It is notable that two of the perhaps most studied sections in the area, including the type locality for the Keel Oolite, include prominent hiatuses, and new studies of other localities and/or core sections in the area are warranted. To tie the Keel Oolite and the Ordovician-Silurian boundary interval of the Arbuckle Mountain area into the global context, it would be feasible to focus on the area of Wapanucka (Johnston County) in the eastern part of the outcrop belt, where the sedimentary succession is more expanded, but where outcrops are lacking and so requiring study of drill cores.

It can be concluded and/or confirmed from this study that:

(1) The Keel Oolite is bounded by major unconformities (sequence boundaries) in the two studied outcrops, although more data are needed to address this for the Sunray DX-Davis 1–5 drill core.

(2) $\delta^{13}C$ data from the Keel Oolite display small variation around largely vertical to weakly positive trend lines. These data are judged as largely reflecting the primary isotopic signal. Thus, this trend, in tandem with the lack of a steep rising or falling trend in the $\delta^{13}C$ data from the Keel Oolite suggests the oolites, locally with abundant pisoids, formed during the peak interval of the HICE. In most successions world-wide, this interval is associated with the middle Hirnantian (middle–upper *M. extraordinarius* and lowermost *M. persculptus* graptolite zones), although it is noted that correlation of the oolites with graptolite biozones is challenging. Brachiopods of the same strata

belong in the Edgewood–Cathay Fauna, suggesting the preserved parts of the oolite belong in the upper part of the *M. persculptus* Zone. This apparent discrepancy may have several reasons and needs more study.

(3) A highly fragmentary and condensed Silurian succession and carbon isotope record is preserved in the Highway 77 road-cut. The fragmented isotope record is corroborated by the previously published conodont biostratigraphy from the area, which suggests several hiatuses in the succession.

(4) For the Silurian strata, integration of carbon isotope stratigraphy with conodont biostratigraphy helps to infer the position of preserved parts of several of the global carbon isotope excursions. Their poor temporal preservation, however, makes them difficult to use for correlation of strata.

Acknowledgements

We wish to thank Nicholas Hayman, Director at Oklahoma Geological Survey, for aiding this research and fieldtrip in several practical ways. The professional help from Vyetta Jordan and colleagues was instrumental for sampling of core sections at OPIC. Jim Barrick is acknowledged for sharing his knowledge and unpublished data from the studied succession. Arbuckle Mountain Fried Pies is acknowledged for helping with practical issues and for providing a sun-shelter and workspace during breaks in the field work. We acknowledge insightful comments from the reviewers Carlton Brett and Andrej Spiridonov. MC acknowledges Bokelunds resestipendiefond (travel grant number RNv-2022-0012) for supporting the research and fieldwork, OL thanks the Deutsche Forschungsgemeinschaft for its support of his stratigraphic work (DFG Le 867/13-1 and 13-2). Birgit Leipner-Mata prepared the large microfacies thin-sections at the Palaeontology Microfacies Lab at Geozentrum Nordbayern in Erlangen. This is a contribution to IGCP 735, "Rocks and the Rise of Ordovician Life – Filling Knowledge Gaps in the Early Palaeozoic Biodiversification".

References

Amsden, T.W. 1957. Stratigraphy and paleontology of the Hunton Group in the Arbuckle Mountain region. Part 1, Introduction to stratigraphy. *Oklahoma Geological Survey Circular 44*, 1–57.

Amsden, T.W. 1959. Stratigraphy and paleontology of the Hunton Group in the Arbuckle Mountain Region. Part VI, Hunton stratigraphy. *Oklahoma Geological Survey Bulletin 84*, 1–311.

Amsden, T.W. 1974. Late Ordovician and Early Silurian articulates brachiopods from Oklahoma southwestern Illinois, and eastern Missouri. *Oklahoma Geological Survey Bulletin 119*, 1–154.

Amsden, T.W. & Barrick, J.E. 1986. Late Ordovician – Early Silurian strata in the central United States and the Hirnantian Stage: *Oklahoma Geological Survey Bulletin 139*, 1–95.

Amsden, T.W., Toomey, D.F. & Barrick, J.E. 1980. Paleoenvironment of Fitzhugh Member of Clarita Formation (Silurian, Wenlockian) Southern Oklahoma. *Oklahoma Geological Survey Circular 83*, 1–54.

Barrick, J.E. & Klapper, G. 1976. Multielement Silurian (late Llandoverian–Wenlockian) conodonts of the Clarita Formation, Arbuckle Mountains, Oklahoma, and phylogeny of *Kockelella*. *Geologica et Palaeontologica 10*, 59–100.

Barrick, J.E., Klapper, G. & Amsden, T.W. 1990. Late Ordovician–Early Devonian conodont succession in the Hunton Group, Arbuckle Mountains and Anadarko Basin, Oklahoma, 55–92. *In* Ritter, S.M. (ed.) *Early to Middle Paleozoic conodont biostratigraphy. Oklahoma Geological Survey Guidebook 27*. University of Oklahoma, Norman.

Barrick, J.E., Kleffner, M.A. & Karlsson, H.R. 2009. Conodont faunas and stable isotopes across the Mulde Event (late Wenlock; Silurian) in southwestern Laurentia (south-central Oklahoma and subsurface west Texas), 41–56. *In* Over, D.J. (ed.) *Conodont Studies Commemorating the 150th Anniversary of the First Conodont Paper (Pander, 1856) and the 40th Anniversary of the Pander Society*. *Palaeontographica Americana 62*.

Barrick, J.E., Klapper, G., Kleffner, M.A. & Karlsson, H.A. 2010a. Conodont biostratigraphy and stable isotope chemostratigraphy of the lower Henryhouse Formation (Gorstian-early Ludfordian, Ludlow, Silurian), southern Oklahoma, USA. *Memoirs of the Association of Australasian Palaeontologists 39*, 51–70.

Barrick, J.E., Kleffner, M.A., Gibson, M.A., Peavey, F.N. & Karlsson, H.A. 2010b. The mid-Ludfordian Lau Event and carbon isotope excursion (Ludlow, Silurian) in southern Laurentia. Preliminary results. *Bollettino della societa Paleontologica Italiana 49*, 13–33.

Bergström, S.M. & Boucot, A.J. 1988. The Ordovician–Silurian boundary in the United States, 273–284. *In* Cocks, L.R.M. & Rickards, R.B. (eds) A *global analysis of the Ordovician–Silurian boundary. Bulletin of the British Museum (Natural History) Geology 43.*

Bergström, S.M. & Goldman, D. 2019. $\delta^{13}C$ chemostratigraphy of the Ordovician–Silurian boundary interval, 145–158. *In* Sial, A.N., Gaucher, C., Ramkumar, M. & Ferreira, V.P. (eds) *Chemostratigraphy across major chronological boundaries*. *American Geophysical Union and John Wiley & Sons Geophysical Monographs 240*.

Bergström, S.M., Saltzman, M.M. & Schmitz, B. 2006. First record of the Hirnantian (Upper Ordovician) δ13C excursion in the North American Midcontinent and its regional implications: *Geological Magazine 143*, 657–678. DOI 10.1017/S0016756806002469

Bergström, S.M., Lehnert, O., Calner, M. & Joachimski, M. 2012. A new Upper Ordovician-Lower Silurian drillcore standard succession from Borenshult in Östergötland, southern Sweden: 2. Significance of $d^{13}C$ chemostratigraphy. *GFF 134*, 39-63. DOI 10.1080/11035897.2012.657231

Bergström, S.M., Eriksson, M.E., Young, S.A., Ahlberg, P. & Schmitz, B. 2014. Hirnantian (latest Ordovician) $\delta^{13}C$ chemostratigraphy in southern Sweden and globally: a refined integration with the graptolite and conodont zone successions: *GFF 136*, 355–386.
DOI 10.1080/11035897.2013.851734

Biebesheimer, E.J., Cramer, B.D., Calner, M., Barnett, B.A., Oborny, S.C. & Bancroft, A.M. 2021. Asynchronous $\delta^{13}C_{carb}$ and $\delta^{13}C_{org}$ records during the onset of the Mulde (Silurian) positive carbon isotope excursion from the Altajme core, Gotland, Sweden. *Chemical Geology 576*, 120256.
DOI 10.1016/j.chemgeo.2021.120256

Brenchley, P.J., Carden, G.A.F., Hints, L., Kaljo, D., Marshall, J.D., Martma, T., Meidla, T. & Nõlvak, J. 2003. High-resolution stable isotope stratigraphy of Upper Ordovician sequences: constraints on the timing of bioevents and environmental changes associated with mass extinction and glaciation. *Geological Society of America Bulletin 115*, 89–104.
DOI 10.1130/0016-7606(2003)115<0089:HRSISO>2.0.CO;2

Brett, C.E., McLaughlin, P.I., Histon, K., Schindler, E. & Ferretti, A. 2012. Time-specific aspects of facies: State of the art, examples, and possible causes. *Palaeogeography, Palaeoclimatology, Palaeoecology 367–368*, 6–18.
DOI 10.1016/j.palaeo.2012.10.009

Calner, M. & Jeppsson, L. 2003. Carbonate platform evolution and conodont stratigraphy during the middle Silurian Mulde Event, Gotland, Sweden. *Geological Magazine 140*, 173–203.
DOI 10.1017/S0016756802007070

Calner, M. & Lehnert, O. 2009. The Hirnantian oolites in Baltoscandia – part of the terminal Ordovician anachronistic period, 5. *In* Harper, D.A.T. & McCorry, M. (eds) *Absolutely final meeting of IGCP 503: Ordovician palaeogeography and palaeoclimate, Copenhagen*. *Abstracts*.

Calner, M., Kozlowska, A., Masiak, M. & Schmitz, B. 2006. A shoreline to deep basin correlation chart for the middle Silurian coupled extinction-stable isotopic event, 79–84. *In* Calner, M. & Eriksson, M.E. (eds) *The Dynamic Silurian Earth*. *GFF 128*. DOI 10.1080/11035890601282079

Carlucci, J.R., Goldman, D., Brett, C.E., Westrop, S.R. & Leslie, S.A. 2015. Katian GSSP and Carbonates of the Simpson and Arbuckle Groups in Oklahoma. *Geology Faculty Publications University of Dayton eCommons 5*, 1–60.

Corradini, C., Corriga, M.G., Männik, P. & Schönlaub, H.P. 2015. Revised conodont stratigraphy of the Cellon section (Silurian, Carnic Alps). *Lethaia 48*, 56–71.
DOI 10.1111/let.12087

Craig, W.W. 1969, Lithic and conodont succession of Silurian strata, Batesville district, Arkansas. *Geological Society of America Bulletin 80*, 1621–1628.
DOI 10.1130/0016-7606(1969)80[1621:LACSOS]2.0.CO;2

Finney, S.C., Berry, W.B.N., Cooper, J.D., Ripperdan, R.L., Sweet, W.C., Jacobson, S.R., Soufiane, A., Achab, A. & Noble, P.J. 1999. Late Ordovician mass extinction: a new perspective from stratigraphic sections in central Nevada. *Geology 27*, 215–218.
DOI 10.1130/0091-7613(1999)027<0215:LOMEAN>2.3.CO;2

Goldman, D. & Bergström, S.M. 1979. Late Ordovician graptolites from the North American Midcontinent. *Palaeontology 40*, 965–1010.

Gul, B., Ainsaar, L. & Meidla, T. 2021. Latest Ordovician–early Silurian palaeoenvironmental changes and palaeotemperature trends indicated by stable carbon and oxygen isotopes from northern *Estonia Estonian Journal of Earth Sciences 70*, 196–209. DOI 10.3176/earth.2021.14

Ham, W.E. 1969. The Geology of the Arbuckle Mountains. *Oklahoma Geological Survey Guide Book* 17, 1–52. The University of Oklahoma University, Norman.

Harper, D.A.T., Hammarlund, E.U., & Rasmussen, C.M.Ø. 2014. End Ordovician extinctions: a coincidence of causes. *Gondwana Research 25*, 1294–1307.
DOI 10.1016/j.gr.2012.12.021

Jeppsson, L., Eriksson, M.E. & Calner, M. 2006. A latest Llandovery to latest Ludlow high-resolution biostratigraphy based on the Silurian of Gotland – a summary. *GFF 128*, 109–114. DOI 10.1080/11035890601282109

LaPorte, D.F., Holmden, C., Patterson, W.P., Loxton, J.D., Melchin, M.J., Mitchell, C.E., Finney, S.C. & Sheets, H.D. 2009. Local and global perspectives on carbon and nitrogen cycling during the Hirnatian glaciation. *Palaeogeography, Palaeoclimatology, Palaeoecology 276*, 182–195.
DOI 10.1016/j.palaeo.2009.03.009

Lemastus, S.W. 1979. *Stratigraphy of the Cason Shale (Ordovician-Silurian), northern Arkansas*. 93 pp. Master thesis, University of New Orleans.

Li, F., Yan, J.X., Burne, R.V., Chen, Z.-Q., Algeo, T.J., Zhang, W., Tian, L., Gan, Y.L., Liu, K. & Xie, S. 2017. Paleo-seawater REE compositions and microbial signatures preserved in laminae of Lower Triassic ooids. *Palaeogeography, Palaeoclimatology, Palaeoecology 486*, 96–107.
DOI 10.1016/j.palaeo.2017.04.005

Lindskog, A., Eriksson, M.E., Bergström, S.M. & Young, S.A. 2019. Lower–Middle Ordovician carbon and oxygen isotope chemostratigraphy at Hällekis, Sweden: implications for regional to global correlation and palaeoenvironmental development. *Lethaia 52*, 204–219. DOI 10.1111/let.12307

McAdams, N.E.B, Cramer, B.D., Bancroft, A.M., Melchin, M.J., Devera, J.A. & Day, J.E. 2018. Integrated $\delta^{13}C_{carb}$, conodont, and graptolite biochemostratigraphy of the Silurian from the Illinois Basin and stratigraphic revision of the Bainbridge Group. *Geological Society of America Bulletin 131*, 335–352. DOI 10.1130/B32033.1

McCracken, A.D. & Barnes, C.R. 1982. Restudy of conodonts (Late Ordovician-Early Silurian) from the Edgewood Group, Clarksville, Missouri. *Canadian Journal of Earth Sciences 19*, 1474–1485. DOI 10.1139/e82-127

McCracken, A. & Lenz, A. 1987. Middle and Late Ordovician conodont faunas and biostratigraphy of graptolitic strata of the Road River Group, northern Yukon Territory. *Canadian Journal of Earth Sciences 24*, 643–653. DOI 10.1139/e87-062

Männik, P. 2007a. Upper Ordovician and lower Silurian conodont biostratigraphy in Estonia: general overview of recent developments. *Estonian Journal of Earth Sciences 56*, 35–46. DOI 10.3176/earth.2007.08

Männik, P. 2007b. An updated Telychian (Late Llandovery, Silurian) conodont zonation based on Baltic faunas. *Lethaia 40*, 45–60. DOI 10.1111/j.1502-3931.2006.00005.x

Munnecke, A. & Männik, P. 2009. New biostratigraphic and chemostratigraphic data from the Chicotte Formation (Llandovery, Anticosti Island, Laurentia) compared with the Viki core (Estonia, Baltica). *Estonian Journal of Earth Sciences 58*, 159–169. DOI 10.3176/earth.2009.3.01

Nõlvak, J., Hints, O. & Männik, P. 2006. Ordovician timescale in Estonia: recent developments. *Proceedings of the Estonian Academy of Sciences, Geology 55*, 95–108. DOI 10.3176/geol.2006.2.02

O'Reilly, S.S., Mariotti, G., Winter, A.R., Newman, S.A., Matys, E.D., McDermott, F., Pruss, S.B., Bosak, T., Summons, R.E. & Klepac-Ceraj, V. 2017. Molecular biosignatures reveal common benthic microbial sources of organic matter in ooids and grapestones from Pigeon Cay, The Bahamas. *Geobiology 15*, 112–130. DOI 10.1111/gbi.12196

Rasmussen, C.M.Ø., Vandenbroucke, T.R.A., Nogues-Bravo, D. & Finnegan, S. 2023. Was the Late Ordovician mass extinction truly exceptional? *Trends in Ecology and Evolution 38*, 812–821. DOI 10.1016/j.tree.2023.04.009

Rong, J., Harper, D.A.T., Huang, B., Li, R., Zhang, X. & Chen, D. 2020. The latest Ordovician Hirnantian brachiopod faunas: New global insights. *Earth-Science Reviews 208*, 103280. DOI 10.1016/j.earscirev.2020.103280

Saltzman, M.R. 2001. Silurian $\delta^{13}C$ stratigraphy: A view from North America. *Geology 29*, 671–674. DOI 10.1130/0091-7613(2001)029<0671:SCSAVF>2.0.CO;2

Satterfield, R. 1971. Conodonts and stratigraphy of the Girardeau Limestone (Ordovician) of southeast Missouri and southwest Illinois. *Journal of Paleontology 45*, 265–273.

Sheehan, P.M. 2001. The Late Ordovician Mass Extinction. *Annual Review of Earth and Planetary Sciences 29*, 331–364. DOI 10.1146/annurev.earth.29.1.331

Simpson, A., Mathieson, D., Frýda, J. & Frýdová, B. 2021. Summary of East Gondwanan conodont data through the Ireviken Event at Boree Creek. *Journal of Earth Science 32*, 512–523. DOI 10.1007/s12583-021-1310-9

Stanley, T.M. 2001. Stratigraphy and facies relationships of the Hunton Group, Northern Arbuckle Mountains and Lawrence uplift, Oklahoma. *Oklahoma Geological Survey Guidebook 33*, 1–74.

Wang, G., Zhan, R., Rong, J., Huang, B., Percival, I.G., Luan, X. & Wei, X. 2017. Exploring the end-Ordovician extinctions in Hirnantian near-shore carbonate rocks of northern Guizhou, SW China: A refined stratigraphy and regional correlation. *Geological Journal 53*, 3019–3029. DOI 10.1002/gj.3140

Yang, X., Li, Z., Fan, T., Gao, Z. & Tang, S. 2020. Carbon isotope ($\delta^{13}C_{carb}$) stratigraphy of the Early–Middle Ordovician (Tremadocian–Darriwilian) carbonate platform in the Tarim Basin, NW China: implications for global correlations. *Geological Magazine 158*, 487–508. DOI 10.1017/S0016756820000643

Zhang, Z., Yang, C., Sahy, D., Zhan, R.-B., Wu, R.-C., Li, Y., Deng, Y., Huang, B., Condon, D.J., Rong, J. & Li, X.-H. 2025. Tempo of the Late Ordovician mass extinction controlled by the rate of climate change. *Science Advances 11*, eadv6788. DOI 10.1126/sciadv.adv6788